 DOI: 10.1002/masy.200750825

Synthesis, Characterization of Copper-Loaded Carboxymethyl-Chitosan Nanoparticles with Effective Antibacterial Activity

*Chunju Gu, Bin Sun, Wenhua Wu, Fengchuan Wang, Meifang Zhu**

Summary: Copper-loaded carboxymethyl-chitosan (CMCS-Cu) nanoparticles were successfully prepared by chelation under aqueous conditions. The effect of degree of deacetylation and substitution, the molecular weight of CMCS, CMCS concentration, Cu(II) ions concentration, pH value of the solution, as well as temperature, on the morphology of the yielded particles were systematically investigated. The physicochemical properties of the particles were determined by size and zeta potential analysis, FTIR analysis, DLS, TEM, SEM and XRD pattern. FTIR and XRD revealed that Cu (II) ions and CMCS formed a chelate complex. The size of CMCS-Cu particles shows a good consistency by DLS, TEM, and SEM. The nanoparticles with the size of about 70 nm have been prepared at 0.13 wt% CMCS, 16 mmol/L Cu(II) ions, pH value 4.56 at 25 °C. The antibacterial activity of CMCS, CMCS-Cu normal particles with the size of about 1000 nm and CMCS-Cu nanoparticles with the size of less than 100 nm against *Staphylococcus aureus* was evaluated by vibration method. Results show that the antibacterial efficiency of nanoparticles reached 99%, which is much more efficient than 68.9% of the normal one and 6.1% of CMCS. CMCS-Cu nanoparticles were proved to be a good novel antibacterial material.

Keywords: antibacterial; carboxymethyl-chitosan; nanoparticle; copper-loaded

1. Introduction

Carboxymethyl chitosan (CMCS), a water-soluble chitosan derivative, has already been used extensively in a wide range of biomedical applications due to its unique chemical, physical, biological properties and its excellent biocompatibility.[1] It is reported that the antibacterial activity of carboxymethyl chitosan depended upon the effective number of $-NH_3^+$ groups in the solution.[2,3]

It was found that[4] the antibacterial activity of CMCS increased significantly with the decrease of molecular weight, e.g. when the molecular weight of CMCS was lower than 5000, CMCS had a very strong antimicrobial action against *Staphylococcus aureus*. But the concentration of microorganism being killed was always more than 1000 ppm. Additionally, CMCS contains hydroxyl (–OH), carboxyl (–COOH) and amine ($-NH_2$) groups in the molecule, and makes it possible to offer enough chelate groups for increasing adsorption capacity toward metal ions. It was also observed that[5] Ag, Zn and Ce loaded CMCS had a good antibacterial activity and the concentration of microorganism being killed could reach several ppm.

Nanoparticles have small particle size and positive surface charges, which may improve their stability in the presence of biological cations and their antibacterial activities due to the interaction with negatively charged biological membranes and site-specific targeting in vivo. It was found

State Key Lab for Modification of Chemical Fibers and Polymer Materials, College of Material Sci. & Eng., Donghua University, Shanghai 201620, China
E-mail: zmf@dhu.edu.cn

Table 1.
DS, DD, Viscometric and Mw of CMCS.

Num.	DS	DD	viscometric	Mw(*1000)
1	0.75	90	100	
2	0.85	90	100	
3	0.95	90	100	
4	0.85	80	100	
5	0.85	95	100	100
6	0.85	90	500	450
7	0.85	90	1000	630

DS, DD and viscometric of CMCS were provided by Shanghai Shengyao Co. Ltd, while Mw was measured by viscometric method.[8]

that chitosan nanoparticles and copper-loaded nanoparticles could inhibit the growth of various bacteria tested.[6]

Up to now no study of copper loaded CMCS nanoparticles has been reported. In an attempt to improve antimicrobial activity of CMCS, our papers report the preparation and characterization of Copper-loaded carboxymethyl-chitosan (CMCS-Cu) nanoparticles. The antibacterial activity of CMCS, CMCS-Cu normal particles with the size of about 1000 nm and CMCS-Cu nanoparticles with the size of less than 100 nm against S*taphylococcus aureus* was also measured by vibration method.

2. Experimental Part

2.1 Materials and Methods

CMCS was supplied by Shanghai Shengyao Co.Ltd., and purified by isoelectric point method.[7] The substitution degree (DS), deacetylation degree (DD), viscometric, molecular weight (Mw) of CMCS were presented in Table 1. $CuSO_4$, HCl, NaOH, and $BaCl_2$ were all analytically pure and obtained from Shanghai Chemicals Co. Ltd., China.

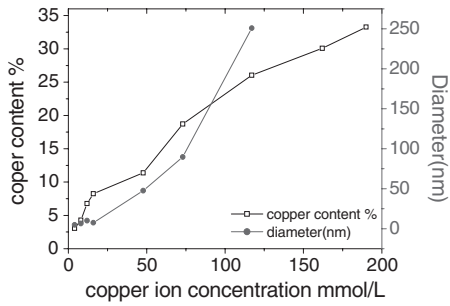

Figure 1.
Effect of Cu(II) ions concentration on the size and copper content of yielded particles(n = 5, CMCS used is num.5 in Table 1).

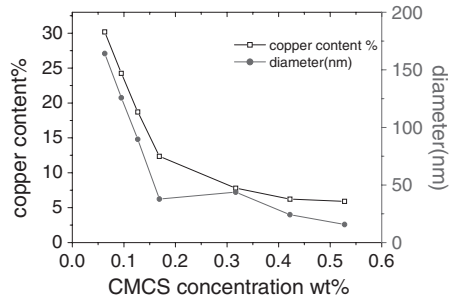

Figure 2.
Effect of CMCS concentration on the size and copper content of yielded particles(n = 5).

2.2 Preparation of CMCS-Cu Nanoparticles

$CuSO_4$ (20 ml) was added into the CMCS solution (100 ml) of certain concentration through flowmeter under magnetic stirring (1000 N/min), and the pH value of the solution was controlled acidly. The yielded particles were purified by centrifugation at 15000 r/min and the solution was moved to measure the Cu(II) ions content. Then the particles were extensively rinsed with distilled water to remove $CuSO_4$ which could be confirmed by $BaCl_2$ solution, and dispersed in distilled water under ultrasonic and lastly spray dried before further use or analysis.

2.3 Characterization

Size Distribution and Zeta Potential(ZP)
Particle size distribution and the zeta potential were determined using Zetasizer Nano-ZS90 (Malvern Instruments). The analysis was performed at a scattering angle of 90° at a temperature of 25 °C using samples diluted to different intensity concentration with de-ionized distilled water.

Fourier Transformed Infrared Spectroscopy(FTIR)
FTIR spectra were taken with potassium bromide pellets on a Nicolet Nexus 670 spectrometer.

Table 2.
Effect of pH on the Size, Zeta Potential(ZP) and Copper Content of Yielded Particles(n = 5).

pH	particle size (nm) (Polydispersity)	ZP(mV)	Cu(II) content%
2.00	13.5 (0.58)	12.96	2.02%
2.84	22.5 (0.48)	14.38	2.18%
3.57	43.8 (0.45)	7.00	4.38%
4.26	58.5 (0.34)	9.49	7.98%
4.86	80.5 (0.30)	18.05	12.86%
5.48	104.2 (0.30)	20.78	19.58%
5.90	178.9 (0.32)	17.48	22.69%
6.10	226.3 (0.42)	16.26	24.92%

X-ray Diffraction(XRD)
X-ray powder diffraction patterns were obtained by a D/max-2550PC diffractometer. The X-ray source was CuKα radiation (18 kw). Samples were scanned at a scanning rate of 4°/min.

Transmission Electron Microscopy(TEM)
Hitachi H-800, operated at 175 kV, was used to study and record the TEM images. The samples were diluted in distilled water and a drop of the diluted liquid was placed and dried on a polymer-coated copper grid.

Scanning Electron Microscopy(SEM)
Morphology studies of CMCS-Cu nanoparticles were carried out using JSM-5600LV scanning electron microscope.

Dynamic Light Scattering (DLS)
The particle size distribution was measured using Brookhaven 90 plus, dynamic light scattering (DLS) spectrometer.

2.4 Evaluation of Antibacterial Activity

According to the ''Disinfection technique standard'' promulgated by ministry of health of P.R.C., vibration method was recommended to evaluate the antibacterial activity of the particles. Evaluation was entrusted by Shanghai Weilai Co. Ltd..

3. Results and Discussion

3.1 Effects of Various Factors on the Morphology of the Yielded Particles

3.1.1 Effects of Cu(II) Ions and CMCS Concentration on the Size and Copper Content of Yielded Particles

It was shown from Figure 1 that the copper content and the size of yielded particles gradually increase with the increase of Cu(II) ions concentration, up to micron size when the Cu(II) ions exceeds 190 mmol/L.

From Figure 2, it was found that with the increase of CMCS concentration in the range of 0.06%–0.53%, the size and copper content of yielded particles gradually decrease, indicating that the increasing speed of copper content is slower than that of CMCS content. Therefore, only under the optimal condition with CMCS of 0.13% and Cu(II) ions of 73 mmol/L CMCS-Cu can be well synthesized.

3.1.2 Effect of pH Value of the Solution on the Size and Copper Content of Yielded Particles

It is mainly carboxyl in CMCS which react with copper to form CMCS-Cu particles while only a few $-NH_2$ and –OH participat-

Table 3.
Effect of DS on the Size, ZP and Copper Content of Yielded Particles(n = 5).

DS	particle size (nm) (Polydispersity)	ZP (mV)	Cu(II) content%
0.75	58.8 (0.21)	11.69	17.18%
0.85	118.1 (0.71)	17.07	24.56%
0.95	*		30.23%

*Insufficient scattering counts.

Table 4.
Effect of DD on the Size, ZP and copper Content of Yielded Particles(n = 5).

DD	particle size (nm) (Polydispersity)	ZP (mV)	Cu(II) content%
0.80	105.7 (0.21)	23.73	20.32%
0.90	118.1 (0.71)	17.07	24.56%
0.95	190.1 (0.41)	12.9	26.51%

ing in the reaction. Nevertheless, since the decomposition of –COOH is restrained and - NH_2 mainly appears as $-NH_3^+$ at strong acidic pH value(ph < 2),[9] the chelate ability of CMCS for Cu(II) ions is weak. In this condition, both of the size and copper content of yielded particles are small. With the increase of pH value, $-COO^-$ and free $-NH_2$ enhance which result in the growth of the size and copper content of yielded particles. Table 2 indicates that when pH value is between 4 and 6, the chelation between CMCS and Cu(II) ions is carried out well and the zeta potential is comparatively high. Additionally, $Cu(OH)_2$ precipitation comes into being if pH value exceeds 5.12 and all Cu(II) ions change into precipitation if pH value exceeds 6.73.[10] Hence the optimal pH value range for the reaction is 4 to 6.

3.1.3 Effect of DS, DD and Mw of CMCS on the Size and Copper Content of Yielded Particles

As seen from Table 3, with the increase of DS of CMCS the size and copper content of yielded particles increase. However, the influence on copper content is nonlinear, which indicates that besides $-COO^-$, –OH, and $-NH_2$ also contribute to the chelation between CMCS and Cu(II) ions. Table 4, 5 indicate that the size and copper content of yielded particles increase with the increase of DD and molecular weight of CMCS.

3.1.4 Effect of Temperature on the Size and Copper Content of Yielded Particles

As seen from Table 6, the size of yielded particles increases and Zeta Potential decreases and becomes unstable as temperature rises. When the temperature is below 50 °C, the copper content of yielded particles increases a bit with the increase of temperature, indicating that chelation is endothermal. On the other hand, when the temperature is above 50 °C, the copper content decreases with the increase of temperature. This phenomenon to some extent accords with Muzzarell's conclusion[11] that when temperature is above 55 °C dechelation will happen resulting in the decrease of copper content. Therefore, combined with Table 6, it was concluded that the optimal reaction temperature is 15–40 °C.

Table 5.
Effect of Mw on the Size, ZP and Copper Content of Yielded Particles(n = 5).

Mw(*1000)	particle size (nm) (Polydispersity)	ZP (mV)	Cu(II) content%
100	68.1 (0.68)	16.75	17.89%
450	118.1 (0.71)	17.07	24.56%
630	168.1 (0.41)	12.87	25.10%

Table 6.
Effect of Temperature on the size, ZP and Copper Content of Yielded Particles(n = 5).

T(°C)	particle size (nm) (Polydispersity)	ZP (mV)	Cu(II) content%
15	80.8 (0.44)	23.12	16.48%
25	89.6 (0.24)	22.34	17.56%
40	105.8 (0.33)	21.15	21.24%
50	158.9 (0.30)	20.81	25.34%
60	209.0 (0.38)	15.43	24.59%
70	496.2 (0.43)	9.59	23.18%

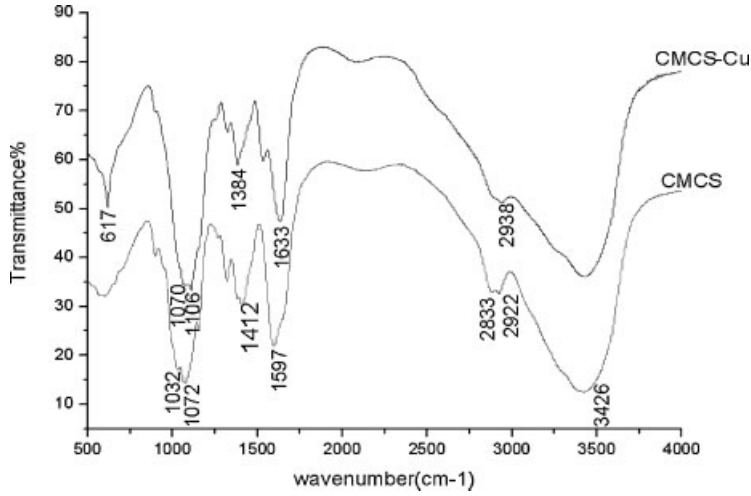

Figure 3.
FTIR Spectra of CMCS-Cu Nanoparticle and CMCS.

3.2 Structure Characterization

3.2.1 FTIR

The spectrum of CMCS-Cu exhibits many alterations from that of CMCS (Figure 3). The major differences are: (1) The adsorption band at 2922 cm^{-1}, assigned to C–H stretching vibration, shows a significant shift to higher wave number (2938 cm^{-1}). The absorbtion band at 1412 cm^{-1}, corresponding to symmetric stretching vibration of C=O shifts to lower wave number. The absorbtion band at 1597 cm^{-1} of the stretching vibration of C=O in $–COO^-$group shifts to 1633 cm^{-1}. These alterations are due to the change of electron cloud density of –COOH which results from the chelation with Cu(II) ions. (2) The absorption band at 1153 cm^{-1}, corresponding to the stretching vibration of C–N bond weakens and shifts to higher wave number, while the wide adsorption band of the stretching vibration of $–NH_2$ and –OH group at 3426 cm^{-1} shifts to the lower wave number. The results indicate the formation of N–Cu bond in the adsorption process. (3) The absorbtion band at 1072 cm^{-1}, due to the stretching of the secondary –C–OH, has a significant shift to 1106 cm^{-1}, which reveals that –OH takes part in the chelation. The band near 617 cm^{-1}, due to the stretching vibration of S–O bond reveals that SO_4^{2-} takes part in the coordination rather than exist as free ion in the complexes.

The results of FTIR analysis show that the carboxyl, amino and secondary hydroxyl groups participate in the formation of the complex, which is in accordance with the study of Sun and Dobetti.[10,12,13]

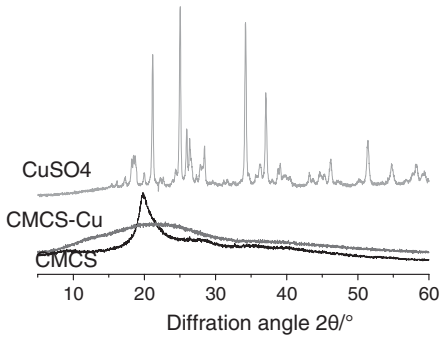

Figure 4.
XRD spectra of CMCS-Cu Nanoparticles, CMCS and $CuSO_4$.

3.2.2 XRD

From Figure 4, the spectrum of $CuSO_4$ exhibits four major crystalline peaks at 2θ 21.2, 25.0, 34.2 and 37.0. Since the DS of CMCS in our experiment is 0.85, only a peak at 2θ 19.1 appears, which is in accordance with Chen.[14] In spectrum of CMCS– Cu the peak at 2θ 19.1 shifts a small angle and becomes even broader and weak.

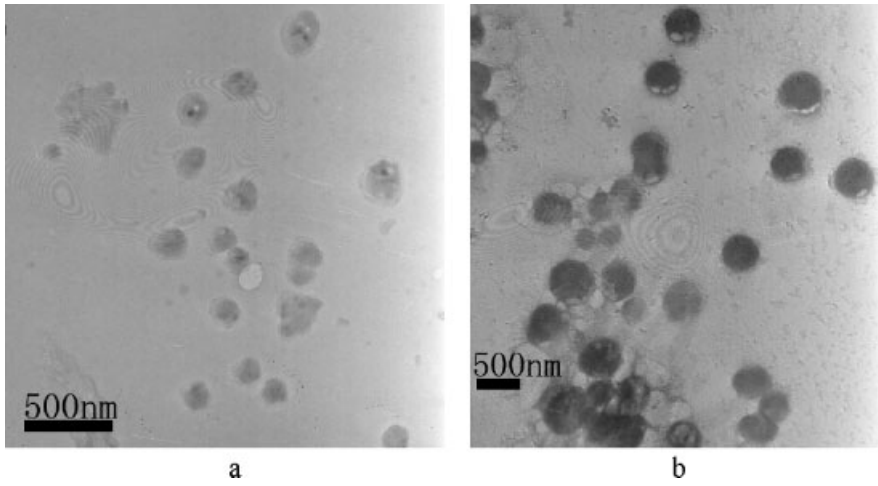

Figure 5.
TEM micrographs of CMCS-Cu nanoparticles. a. CMCS = 0.13%, [Cu(II) ions] = 73 mmol/L, pH = 4.95, T = 25 °C, b. CMCS = 0.13%, [Cu(II) ions] = 117 mmol/L, pH = 4.95, T = 25 °C.

Hence, the hydrogen bond in CMCS has been destroyed by chelation, so as to obtain amorphous CMCS-Cu.

From FTIR, XRD and the experiments analyses, the structure of CMCS-Cu can be deduced as a chelate complex.

3.2.3 TEM and SEM

CMCS-Cu nanoparticles as shown in Figures 5 and 6 by TEM and SEM observation exhibit regular shapes like balls under optimal reaction conditions, and the sizes apparently increase with the increase of Cu(II) ions concentration.

3.2.4 DLS

It is seen from Figure 7 that the size of CMCS-Cu particles yielded under optimal reaction conditions is between 13 to 496 nm, most of which are about 100 nm. This result consists with that of TEM and SEM.

3.3 Evaluation of Antibacterial Activity

The antibacterial activities of CMCS, CMCS-Cu normal particles with the size of about 1000 nm and CMCS-Cu nanoparticles with the size of less than 100 nm against *Staphylococcus aureus,* a typical

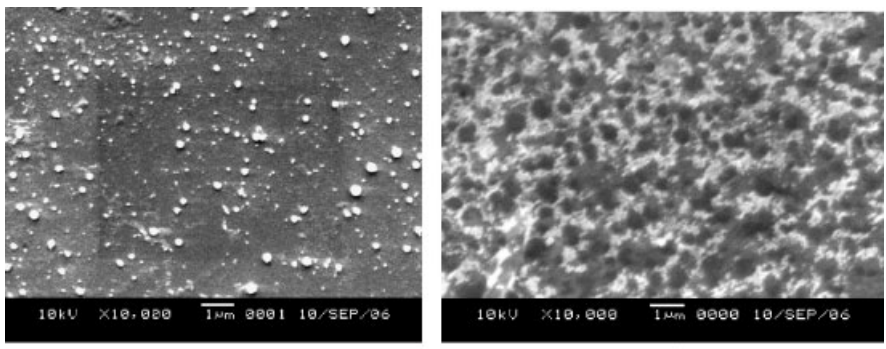

Figure 6.
SEM micrographs of CMCS-Cu nanoparticles. a. CMC = 0.13%, [Cu(II) ions] = 73 mmol/L, pH = 4.95, T = 25 °C. b. CMC = 0.13%, [Cu(II) ions] = 117 mmol/L, pH = 4.95, T = 25 °C.

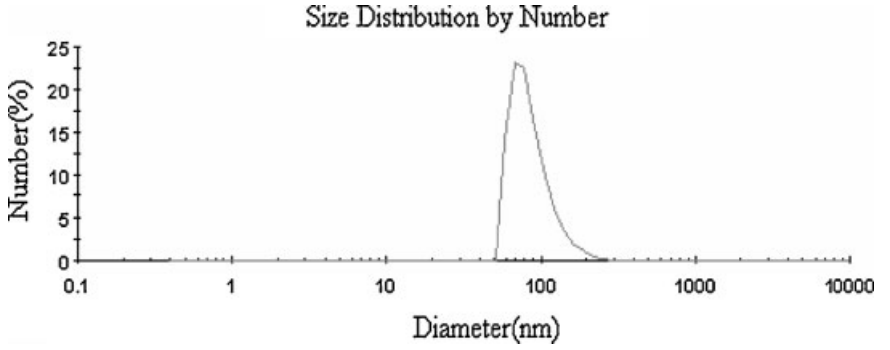

Figure 7.
CMCS-Cu nanoparitcles size distribution by number (CMC = 0.13%, [Cu(II) ions] = 73 mmol/L, pH = 4.95, T = 25 °C).

Table 7.
Antibacterial Activity of CMCS, CMCS-Cu Normal Particles and Nanoparticles.

Material	Average size of material	Antibacterial efficiency against *Staphylococcus aureus*
CMCS	–	6.1%
CMSC-Cu normal particles	About 1000 nm	68.9%
CMSC-Cu nanoparticles	<100 nm	99%

Gram-positive bacterium, are shown in Table 7. Results show that the antibacterial efficiency of nanoparticles reached 99%, which is much more efficient than the normal one of 68.9% and CMCS of 6.1%. These indicate that CMCS-Cu nanoparticles prepared by chelation have a good antibacterial ability.

4. Conclusion

CMCS-Cu nanoparticles were successfully prepared by chelation of CMCS and Cu(II)ions. Through a number of tests, we found that the nanoparticles with the size of about 70 nm can be prepared at 0.13wt% CMCS, 16 mmol/L Cu(II) ions, pH value 4.56 at 25 °C. The antibacterial efficiency of CMCS-Cu nanoparticles against *Staphylococcus aureus* reached 99%, which was much more efficient than that of the normal one and CMCS. CMCS-Cu nanoparticles were proved to be a good novel antibacterial material.

Acknowledgements: We are grateful for the financial support of this research from *Shanghai Key Fundamental Foundation (06JC14003)* and *the Shanghai Nano Special Projects (0552nm005).*

[1] N. V. Majeti, Ravi Kumar, *Reactive and Functional Polymers*, **2000**, *46*(1), 1–27.
[2] L. P. Sun, Y. M. Du, L. H. Fan, X. Chen, J. H. Yang, *Polymer*, **2006**, *47*(6), 1796–1804.
[3] F. L. Xiao, L. G. Yun, Z. Y. Dong, L. Zhi, D. Y. Kang, *J. Appl. Polym. Sci.* **2001**, *79*, 1324–1335.
[4] L. Y. Chen, Y. M. Du, Y. Liu, *J. W uhan U niv. (Nat. Sci. Ed., in Chinese)* **2000**, *46*(2), 191–194.
[5] Y. Z. Xiong, X. J. Zhan, Z. Liu, *Pharmaceutical Biotechnology*, **2004**, *11*(6), 361–363.
[6] L. F. Qi, Z. R. Xu, X. Jiang, C. H. Hu, X. F. Zou, *Carbohyd. Res.* **2004**, *339*(16), 2693–2700.
[7] C. Zhong, J. Zhao, M. Z. Huang, *Fine Chemicals(in Chinese)*, **2004**, *21*(5), 338–341.
[8] G. A. F. Roberts, J. G. Domszy *Int. J. Biol. Macromol.* **1982**, *4*(6), 374–377.
[9] L. Dobetti, F. Delben, *Carbohyd. Polym.* . **1992**, *18*(4), 273–282.
[10] S. L. Sun, A. Q. Wang, *Sep. Purif. Technol.* **2006**, *49*(3), 197–204.
[11] R. A. A. Muzzarelli, M. Weckx, O. Filippini, F. Sigon, *Carbohyd. Polym.* **1989**, *11*(4), 293–306.
[12] S. L. Sun, A. Q. Wang, *J. Hazard Mater* **2006**, *131*(1–3), 103–111.
[13] L. Dobetti, F. Delben, *Carbohyd. Polym,.* **1992**, *18*(4), 273–282.
[14] L. Y. Chen, Y. M. Du, X. Q. Zeng, *Carbohyd. Res.* **2003**, *338*(4), 333–340.

